Original Article

Diffusion-weighted images (DWI) without ADC values in assessment of small focal nodules in cirrhotic liver

Mai-Lin Chen, Xiao-Yan Zhang, Li-Ping Qi, Qing-Lei Shi, Bin Chen, Ying-Shi Sun

Key Laboratory of Carcinogenesis and Translational Research (Ministry of Education), Department of Radiology, Peking University Cancer Hospital & Institute, Beijing 100142, China

Corresponding to: Yingshi Sun. Key Laboratory of Carcinogenesis and Translational Research (Ministry of Education), Department of Radiology, Peking University Cancer Hospital & Institute, No.52 Fucheng Road, Haidian District, Beijing 100142, China. Email: sunysabc@163.com.

Objective: To assess if diffusion-weighted magnetic resonance (MR) imaging without apparent diffusion coefficient (ADC) values provides added diagnostic value in combination with conventional MR imaging in the detection and characterization of small nodules in cirrhotic liver.

Methods: Two observers retrospectively and independently analyzed 86 nodules (≤3 cm) certified pathologically in 33 patients with liver cirrhosis, including 48 hepatocellular carcinoma (HCC) nodules, 13 high-grade dysplastic nodules (HDN), 10 low-grade dysplastic nodules (LDNs) and 15 other benign nodules. All these focal nodules were evaluated with conventional MR images (T1-weighted, T2-weighted and dynamic gadolinium-enhanced images) and breath-hold diffusion-weighted images (DWI) (b=500 s/mm^2). The nodules were classified by using a scale of 1-3 (1, not seen; 3, well seen) on DWI for qualitative assessment. These small nodules were characterized by two radiologists. ADC values weren't measured. The diagnostic performance of the combined DWI-conventional images and the conventional images alone was evaluated using receiver operating characteristic (ROC) curves. The area under the curves (Az), sensitivity and specificity values for characterizing different small nodules were also calculated.

Results: Among 48 HCC nodules, 33 (68.8%) were graded as 3 (well seen), 6 (12.5%) were graded as 2 (partially obscured), and 9 weren't seen on DWI. Among 13 HDNs, there were 3 (23.1%) and 4 (30.8%) graded as 3 and 2 respectively. Five (50%) of 10 benign nodules were partially obscured and slightly hyperintense. For 86 nodules, the average diagnostic accuracy of combined DWI-conventional images was 82.56%, which was increased significantly compared with conventional MR images with 76.17%. For HCC and HDN, the diagnostic accuracy of combined DWI-conventional images increased from 78.69% to 86.07%.

Conclusions: Diffusion-weighted MR imaging does provide added diagnostic value in the detection and characterization of HDN and HCC, and it may not be helpful for LDN and regenerative nodule (RN) in cirrhotic liver.

Keywords: Diffusion-weighted imaging; magnetic resonance (MR) imaging; cirrhosis; nodule

Submitted Sep 15, 2013. Accepted for publication Dec 04, 2013.
doi: 10.3978/j.issn.1000-9604.2014.01.07
Scan to your mobile device or view this article at: http://www.thecjcr.org/article/view/3342/4175

Introduction

Cirrhosis is a progressive diffuse process of liver fibrosis that is characterized by architectural distortion and the development of a spectrum of nodules ranging from benign regenerative nodule (RN), low-grade dysplastic nodule (LDN), and high-grade dysplastic nodule (HDN) to overtly malignant hepatocellular carcinoma (HCC) nodules. The decision to proceed to treat is based on the number and size of lesions. Thus, therapies are increasingly depending on accurate analysis from radiologists focused on the exact number, location and characterization of nodular lesions in cirrhotic liver. Radiologists have used computed tomography (CT) during arterioportography and conventional magnetic resonance (MR) imaging, which

involves T1-weighted, T2-weighted, and dynamic enhanced T1-weighted imaging by now to evaluate the liver nodules.

Recent results (1-5) have shown that diffusion-weighted images (DWI) can help characterize focal nodular lesions. However, the utility and diagnostic accuracy of DWI for the detection of RN, LDN, HDN and HCC in cirrhotic liver have not been widely reported. Furthermore, the additional value of DWI without apparent diffusion coefficient (ADC) values to conventional MR imaging in different cirrhosis-related nodules is still unknown.

So, the aim of our study was to determine whether DWI without ADC values provides added diagnostic value in combination with conventional MR imaging in the detection and characterization of different nodules associated with cirrhosis.

Materials and methods

Patients

Our MR imaging database was retrospectively searched to identify patients who underwent T1-weighted, T2-weighted, dynamic enhanced and diffusion-weighted MR imaging of the liver between September 2006 and October 2010. Patient inclusion criteria included: (I) pathologically proven livercirrhosis; (II) at least one focal liver lesion detected by MR imaging; and (III) the diameter of measured nodules was smaller than 30 mm in axial images. Those who do not meet any one of the above were excluded (12 patients were excluded). Hence, the final study population was composed of 33 patients (27 males, 6 females), with a mean age of 55.6 years (range, 36 to 82 years). Cirrhosis was caused by hepatitis B in 25 patients, hepatitis B and alcoholism in 2, alcoholism in 2, hepatitis C in 1, steatosis in 1, and primary biliary cirrhosis in 1. The cause of cirrhosis was cryptogenic in one patient. All patients, except those with primary biliary and cryptogenic cirrhosis, had Child-Pugh class B (12 cases) or Child-Pugh class C (19 cases).

MR imaging

Patients were examined with a 1.5 T superconducting MR imager (Gyroscan; Philips Medical Systems, Best, the Netherlands) and a SENSE body coil. All patients were performed with diffusion-weighted MR imaging in addition to imaging with a routine hepatic MR protocol. The protocol included a T1-weighted dual fast gradient-recalled-echo sequence (in-phase and out-of-phase sequences) [repetition time ms/echo time ms, 126/4.6 (in-phase), 2.3 (out-of-phase); flip angle, 80°; matrix, 512×256; section thickness, 7 mm; intersection gap, 1 mm; one signal acquired; field of view, 320 mm], a transverse T2-weighted fast spin-echo sequence with spectral fat saturation (4,062/90; fast spin-echo factor, 15; matrix, 512×256; section thickness, 7 mm; intersection gap, 1 mm; two signals acquired; field of view, 320 mm).

Breath-hold axial diffusion-weighted SENSE imaging was performed prior to contrast administration: repetition time ms/echo time ms, 1,850/56; *b* factors, 500 s/mm^2; spectral pre-saturation with inversion recovery for fat suppression; matrix size, 256×256; reduction factor of SENSE, two; field of view, 320 mm; section thickness, 7 mm; section gap, 1 mm; the entire liver (from the level of the diaphragm to the inferior edge of liver) was typically evaluated in two to three breath-holds.

Dynamic T1-weighted imaging, gradient-echo out-of-phase sequence with 2D acquisition: 7 mm slice thickness, repetition time ms/echo time ms, 126/2.3; flip angle, 80°; matrix, 512×256; intersection gap, 1 mm; field of view, 320 mm, before and after dynamic injection of 0.1 mmol per kilogram of body weight of gadopentetic acid dimeglumine (Magnevist; Bayer Schering Pharma AG, Guangzhou, China) or gadopentetate dimeglumine (Magnevist; Beilu Pharmaceutical Co., Ltd., Beijing, China) through a power injector at a rate of 2 mL/s, followed by a 20 mL saline flush. To determine the time for hepatic arterial phase, a 1 mL test bolus of contrast material was administered to determine the time to peak arterial enhancement. Then the same sequence was repeated immediately (20-30 min).

All sequences covered the whole liver. The section thickness, section gap, and field of view were occasionally changed depending on the size of the liver. The only preparation before the examination was an 8-hour fasting period. During the image acquisition phase of the (I) T2-weighted fast spin-echo; (II) dual-echo T1-weighted imaging; and (III) T2-weighted MR imaging sequences, oxygen inhalation was provided to make it easier for the patient to hold breath longer.

Image analysis

Two observers (each with 10 and 15 years of experience in abdominal MR imaging) retrospectively and independently reviewed conventional MR images (T1-weighted, T2-weighted and Dynamic T1-weighted images) and combined DWI-conventional images on a commercially available workstation (Advantage Workstation; GE Medical

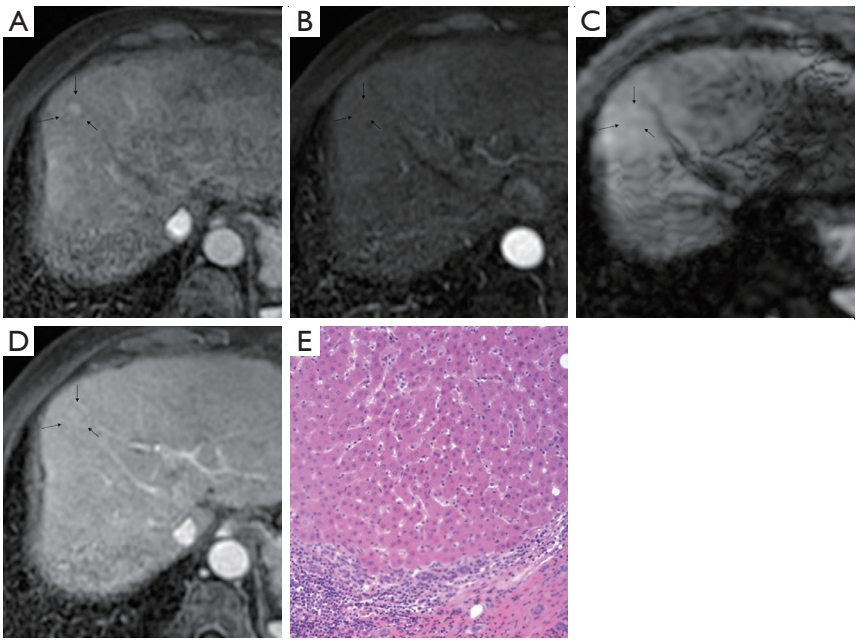

Figure 1 MR images in a 62-year-old man with liver cirrhosis and RN in right lobe. Small RN (arrows) was identified on the second dynamic enhanced T1-weighted images (A), but was not visualized on arterial-phase enhanced images (B); (C) The transverse DWI at b=500 s/mm^2; (D) The any subsequent enhanced images; The photograph of histological specimen (E) shows a nodule with no atypia and normal nuclear-cytoplasmic ratio.

Systems) respectively. The observers were blinded to the initial clinical MR interpretations and biopsy results, and only recorded nodular lesions smaller than 30 mm. The nodule information included location, size, number, and corresponding liver segment noted for diffusion-weighted imaging and conventional MR images.

Images were analyzed in two sessions. At first, the observers reviewed the conventional MR images: T1-weighted dual fast gradient-recalled-echo sequence (in-phase and out-of-phase sequences), T2-weighted fast spin-echo sequence and dynamic T1-weighted images with multiple phases. After 4-6 weeks, the observers reviewed the combined DWI-conventional images: T1-weighted images (in- and out-of-phase), T2-weighted fast spin-echo, dynamic images with fat saturation, and DWI. The observers were always asked to identify all nodular lesions in cirrhotic liver and characterize them by using a 5-point scale: (1, definitely benign; 2, probably benign; 3, may or may not be malignant; 4, probably malignant; and 5, definitely malignant). Benign discreet nodular lesions that fulfilled all or most of imaging criteria for cysts, hemangiomas, and RNs and LDNs (6-8) were assigned a score of 1, 2 or 3. Malignant nodular lesions with some or all features (8-10) suggestive of malignancy were assigned a score of 4 or 5. These features suggestive of malignancy included lesion hypointensity compared with the prior enhancement nodule on subsequent contrast enhanced images (classified as "washout") (*Figure 1*), lesion of enhancement in arterial phase that become isointense or remain mildly hyperintense compared with liver parenchyma in subsequent phases (11) (classified as "arterial enhancement") (*Figure 2*), lesion of rim enhancement on any postcontrast enhanced images (12) (classified as "rim enhancement") (*Figure 3*), or lesion with high signal intensity on the DWI based on the appearance of "washout" (13-16) (*Figure 4*).

And then, observers 1 and 2 assessed the conspicuity of all discreet histologically-proven lesions on diffusion-weighted MR images by using a scale of 1-3 (1, not seen; 2, partially obscured; and 3, well seen) (*Figures 1-4*) in consensus. The observers recorded the signal intensity of all histologically-proven nodular lesions compared with liver parenchyma on the DWI.

Among all visible lesions, there were 86 lesions proved by histology at 5-10 weeks of intervals between imaging and surgery. Seventy nodular lesions in 24 liver transplantation recipients were determined by one pathologist with ten

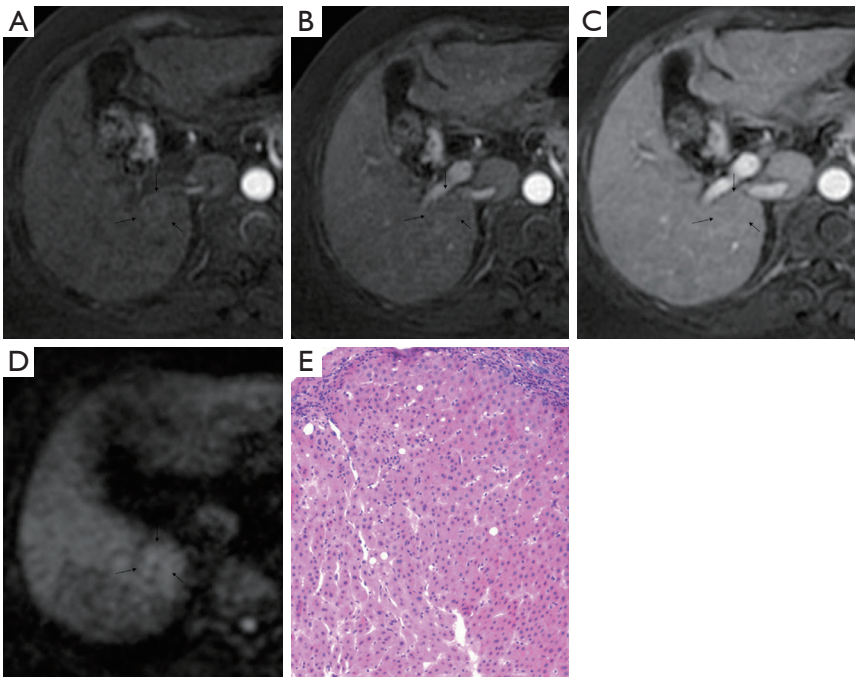

Figure 2 MR images in a 61-year-old woman with liver cirrhosis and LDN in right lobe. Nodular dysplasia (arrows) was mildly enhanced on the arterial-phase enhanced images (A), but was not visualized on the subsequent dynamic enhanced T1-weighted images (B and C); It was obscured on the transverse DWI at b=500 s/mm^2 images (D); The picture of histological specimen (E) shows a nodule with mild atypia and slightly increased nuclear-cytoplasmic ratio.

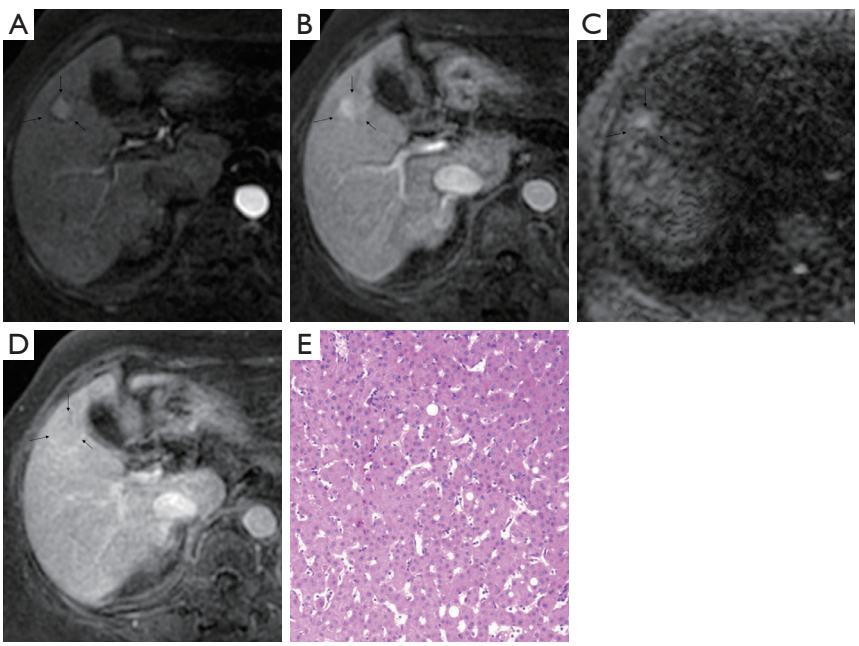

Figure 3 MR images in a 68-year-old woman with liver cirrhosis and HDN. The lesion (arrows) was enhanced on transverse arterial-phase enhanced images (A) and transverse portal-phase enhanced images (B), and was shown mildly hyperintense on transverse DWI (b=500 s/mm^2) (C); It was not seen on T1-weighted delayed-phase images (D); The photograph of histological specimen (E) shows a nodule with moderate atypia and higher nuclear-cytoplasmic ratio.

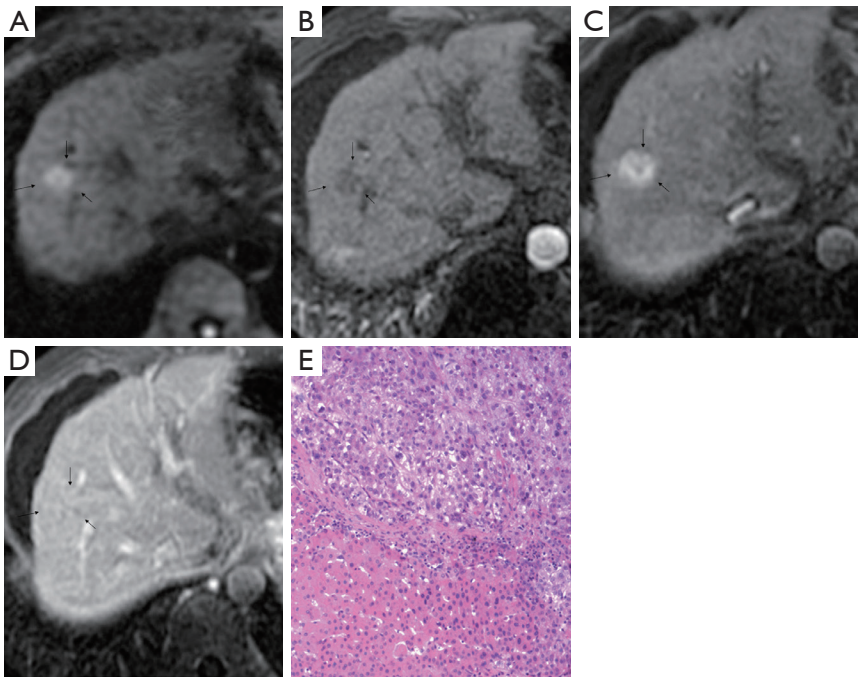

Figure 4 MR images in a 53-year-old man with liver cirrhosis and HCC. The transverse DW (b=500 s/mm^2) images (A) demonstrates the lesion with hyperintensity (arrows), which was not enhanced on transverse arterial-phase enhanced images (B), but was identified on transverse subquent enhanced images (C); It was not detected on T1-weighted delayed-phase images (D) either; The picture of histological specimen (E) shows a malignant neoplasm with obvious atypia and hepatocellular differentiation.

years of experience, who cut the explanted livers sequentially into 5-8 mm sections that corresponded as closely as possible to the MR images. Four lesions of three patients were obtained by biopsy, ultrasound (US)-guided biopsy was performed in correlation to the imaging findings, and the segmental location of the biopsied lesion was noted. Twelve lesions of six patients confirmed with surgical resection were located by intraoperative US in correlation to the imaging results prior to resection. Subsequently, similarly as for whole-explant evaluation, every lesion was macroscopically examined by the pathologists.

All available imaging and pathologic findings were independently re-reviewed and evaluated by another radiologist. Nodular lesions not visible on conventional MR images or DWI were classified as "definitely not be malignant" (score =1). Receiver operating characteristic (ROC) curves were constructed based on observer's scoring of nodular lesions using each session and the areas under the curves (Az) were calculated.

Statistical analysis

ROC analysis was performed for analysis of the 86 nodular lesions with pathologically proved findings using MedCalc (MedCalc Inc., Merienke, Netherlands). The overall diagnostic accuracy of each session was determined by comparing with histopathology. The Az was calculated and pairwise comparison was made between session 1 and session 2 within observers using the variance Z-test. Interobserver agreement in lesion scoring was determined using kappa statistics. Kappa values of <0.20 indicated poor agreement, 0.21-0.40 slight agreement, 0.41-0.60 moderate agreement, 0.61-0.80 good agreement, and >0.81 very good agreement.

Results

Lesion detection

Thirty-three patients with known cirrhosis underwent MR examination. Among 86 histologically-proven lesions detected at the consensus reading, there were 48 HCCs, 13 HDNs, 10 LDN and RNs, 6 hemangiomas and 9 cysts. Lesions varied in diameter from 5 to 30 mm (mean 13 mm). Besides, because of the inability to differentiate HDNs from HCC at imaging and because of the likelihood that

Table 1 Reader confidence rankings of benign and malignant lesions

Lesion type and session No.	Reader 1 score*					Reader 2 score*				
	1	2	3	4	5	1	2	3	4	5
Benign										
1	10	8	3	2	2	9	8	5	2	1
2	11	8	3	2	1	10	8	4	2	1
Malignant										
1	2	4	6	19	30	2	5	7	18	29
2	1	2	5	18	35	0	3	6	17	35

*, a score of 1 represents "definitely benign", and a score of 5 represents "definitely malignant".

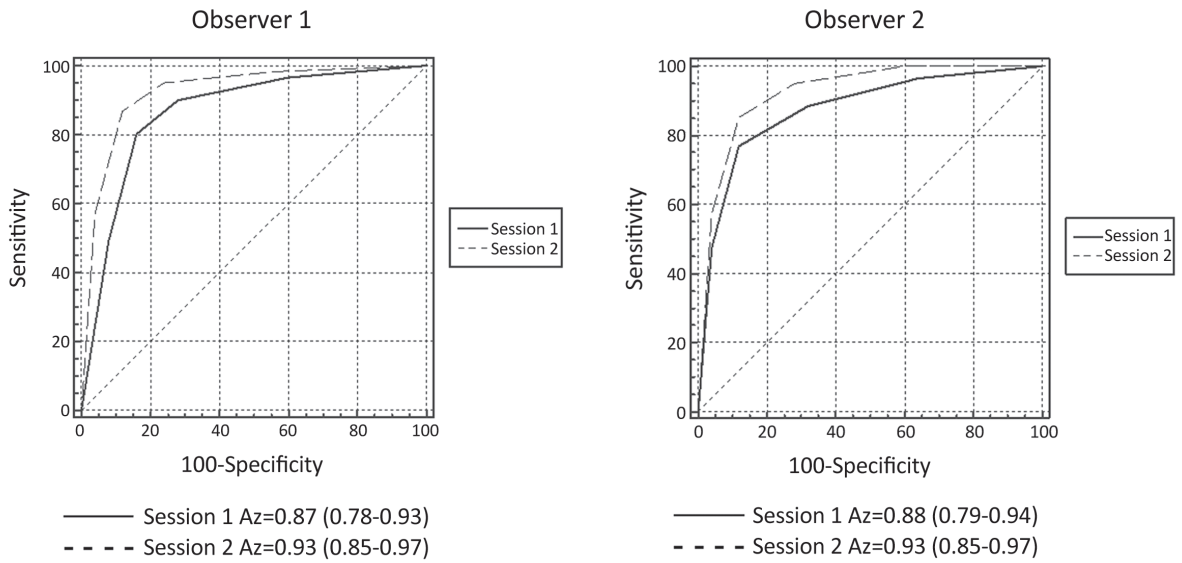

Figure 5 ROC curves for the detection of nodular lesions using Session 1 and Session 2. The Az is shown with 95% CI.

HDNs will transform into HCC, HDNs were assigned in the analysis as malignant lesions (8).

Lesion characterization

Observer rankings of benign and malignant nodules are shown in *Table 1*. ROC curves for two observers and Az are shown in *Figure 5*. Diagnostic sensitivity and specificity of individual observers in detecting nodular lesions in cirrhotic liver using Session 1 and Session 2 are noted in *Table 2*. Comparison within same observer, for observer 1, the diagnostic accuracy of session 2 [83.72%, Az=0.93; 95% confidence interval (95% CI): 0.85-0.97] was significantly higher than session 1 (77.91%, Az=0.87; 95% CI: 0.78-0.93) (P=0.001). For observer 2, there was also significant difference between session 1 (74.42%, Az=0.88; 95% CI: 0.79-0.94) and session 2 (81.40%, Az=0.93, 95% CI: 0.85-0.97) (P=0.004). However, there was no significant difference about the diagnostic accuracy between two observers in session 1 (P=0.16) and session 2 (P=0.93). And a very good interobserver agreement existed in classifying the focal liver lesions into categories 1-5 using conventional MR imaging and combined DWI-conventional MR imaging (in session 1, kappa =0.68; 95% CI: 0.60-0.76; in session 2, kappa =0.73; 95% CI: 0.67-0.79).

Detection rate of 86 histologically-proven nodules by Session 1 and Session 2 is shown in *Table 3*. DWI combined with conventional MR imaging was associated with a significantly higher detection rate of HCC and HDNs [HCC: 47 of 48 (97.9%) *vs*. 45 of 48 (93.8%); HDN: 11 of 13 (84.6%) *vs*. 8 of 13 (61.5%); P<0.001]. When the detection performance of both observers were averaged,

Table 2 Diagnostic sensitivity and specificity of individual observers in detecting nodular lesions in cirrhotic liver using Session 1 and Session 2

Session	Observer 1			Observer 2		
	Sensitivity	Specificity	Az	Sensitivity	Specificity	Az
Session 1	0.80	0.84	0.87	0.77	0.86	0.88
Session 2	0.87	0.88	0.93	0.85	0.88	0.93
P			0.001			0.004

Score of 4 or more indicates malignant.

Table 3 Detection rate of 86 histologically-proven nodules by Session 1 and Session 2

Session	All nodules	HCC	HDN	LDN + RN	Other
Session 1	87.5 (75/86)	93.8 (45/48)	61.5 (8/13)	70.0 (7/10)	86.7 (13/15)
Session 2	93.0 (80/86)	97.9 (47/48)	84.6 (11/13)	65.5 (6.5/10)	93.3 (14/15)
P	<0.001	<0.001	<0.001	>0.05	<0.001

Data are averaged for two independent observers. Unless otherwise indicated, numbers are percentages, with raw data in parentheses.

Table 4 Lesion characterization of 86 biopsy-proved nodules in comparison to liver parenchyma

Nodule	Enhancement type of dynamic T1WI				DWI conspicuity		
	Arterial	Washout*	Rim	No**	1	2	3
HCC (n=48)	20	15	10	3	9	6	33
HDN (n=13)	5	4	1	3	6	4	3
LRN*** (n=10)	5	2	0	3	5	5	0
Other**** (n=15)	7	3	3	2	2	5	8

Data are numbers of nodular lesions. *, nodules here didn't include lesions with "enhanced in arterial phase" and "rim enhancement"; **, no enhancement compared with liver parenchyma; ***, low-grade dysplastic (LDN) and regenerative nodules (RNs); ****, 6 hemangiomas and 9 cysts.

the number of LDN and RN detected with combined DWI-conventional images [LDN: 6.5 of 10 (70%)] wasn't significantly greater than that with conventional MR images alone [7 of 10 (70%)] (P>0.05). Besides, compared with conventional MR images, there was no increase of accuracy rate of hemangiomas and cysts detected with combined DWI-conventional images [14 of 15 (93.3%) *vs.*13 of 15 (86.7%), P>0.05].

The signal intensity and enhancement type of all 86 histologically proven nodules in cirrhotic liver are shown in *Table 4*. Twenty of 48 (41.7%) HCCs were enhanced obviously on arterial-phase images, 15 of 48 (31.3%) were "washout", and 10 of 48 (20.8%) were "rim enhancement". These nodules with "arterial enhancement" and "rim enhancement" showed lower signal intensity compared with the higher intensity of prior enhancement on subsequent contrast enhanced images, and had the same type of "washout". All in all, most of nodules (93.8%, 45/48) were "washout" in cirrhotic liver, as mentioned previously. Besides, 9 of 13 HDNs in cirrhosis had the similar appearance (*Figure 3*). Interestingly, 1 LDN and 1 RN were also detected with lower signal intensity compared with prior enhancement on dynamic T1-weighted images (*Figures 1*,*2*).

On diffusion-weighted MR images, 44 of 86 (51.2%) histologically proven lesions were graded as 3 (well seen), 20 (23.3%) were graded as 2 (partially obscured), and 22 (25.6%) were graded as 1 (not seen). Thirty-three of 48 HCCs nodules were obvious hyperintense compared with liver parenchyma on DWI, 6 HCCs were mild

hyperintense, and others were iso- or hypo-intense. In 13 HDNs, there were 4 nodules with mild hyperintense and 3 nodules with high signal intensity detected on DWI. Two of 4 LDNs and 3 of 6 RNs were mild hyperintense on DWI compared with surrounding hepatic tissue. Hepatic cysts were demonstrated with various signal intensities on DWI (2 hyperintense, 2 mild hyperintense), although they had the shared characteristic of demonstrating low signal intensity on DWI (5 hypointense). Four hemangiomas were hypointense and 2 hemangiomas were hyperintense.

Discussion

One of the key challenges to liver imaging in cirrhotic patients is the ability to accurately define the nodule presence and its characterization. Now, dynamic contrast enhanced MR imaging is a more appropriate imaging procedure for the detection of liver nodules (17). While arterial enhancement is the most consistent feature of HCC (18), it is by no means a specific feature. In our study, 12 of 25 (48%) benign nodules enhanced in the arterial phase, including 5 RNs, and 7 of 14 non-cirrhotic nodules (6 hemangiomas and 1 post-infected cyst). Similar appearance had ever been reported in other benign and malignant lesions in cirrhotic liver (19). However, as mentioned before, we found the feature of "washout" got up to 93.8% (45/48) in HCCs and 9 of 13 (69.3%) in HDNs in cirrhotic liver, which is more frequent than that of "arterial enhancement" reported above. Although 3 arterial enhancing HDNs and 1 LDN were falsely diagnosed as HCC in our study, it is a little difficulty to differentiate all arterial enhancing HCCs, dysplastic and regenerative nodules (RNs) (9,18,20). We thought that it was a malignant nodule if a nodule presented the feature of "washout" in cirrhotic liver.

Diffusion is a Brownian motion that describes the microscopic random movement of molecules in response to thermal energy. It may be affected by the biophysical properties of tissues such as cell organization and density, microstructure, and microcirculation. Diffusion pulse sequences and techniques are sensitive to very small-scale motion of water protons at the microscopic level. DWI is utilized to provide very rapid imaging that is sensitive to subtle small-scale alternations in diffusion. Areas of restricted water diffusion are displayed as areas of high signal intensity. Investigators in several studies have compared the utility and accuracy of diffusion-weighted and dynamic enhanced MR sequences in focal liver lesions, with consensus results (1,13-16,21-23) that favoring diffusion-weighted imaging with ADC values improved detection of focal nodular lesions. In our study, 39 (81.3%) of HCCs were hyperintense compared with liver parenchyma on DWI, that means diffusion of biophysical tissues had altered, and motion of water protons had been restricted. Most of them (33/39) showed significant hyperintensity, demonstrated to be malignant. Seven of 13 HDNs were also hyperintense compared with liver parenchyma, indicating alternations in diffusion of biophysical tissues. Two of them were verified focal malignant transformation at the corresponding areas. Combined DWI with conventional MR imaging showed much better than conventional MR imaging alone for the detection of HCCs and HDNs in cirrhotic patients. Therefore, DWI may aid in diagnosing HDNs and HCC. Besides, DWI plus ADC values may favor in distinguishing HDN from HCC for their different pathologic changes of HDN and HCC (15). But in this study, ADC values weren't calculated. Because the size range of ADC values reported in recent studies (24-27) was inconsistent or conflicted, the use of equipments, *b* values, measurement methods etc., used in these reported studies, were different. It is difficult to obtain a uniform or applicable ADC value in current clinical practice. Therefore, we think that it is reasonable and feasible to observe the signal intensity of lesions on DWI in medical work.

Five of 10 of LDNs and RNs in our study were mild hyperintense on DWI compared with surrounding hepatic tissue, including 2 of 4 LDNs, 3 of 6 RNs, and none of them was notable hyperintense. DWI combined with dynamic T1WI wasn't associated with a significantly higher detection rate of both LDN and RN. So, it was hard to say that DWI aids in detection of small LDNs and RNs compared with dynamic contrast-enhanced T1WI alone. The likely explanation for LDN or RN with mild hyperintensity was local areas of active fibrosis or infarction.

In addition, the accuracy rate of other nodules (hemangiomas and cysts) detected by DWI and dynamic T1WI wasn't significantly higher than that by dynamic T1WI. For most of these nodules, low signal intensity in T1-weighted images, high signal intensity in T2-weighted images and typical type of enhancement in dynamic T1WI were also helpful to diagnose hemangiomas and cysts.

However, DWI is sensitive to motion, susceptibility and ghosting artifacts. In our study, 9 lesions of 48 HCC nodules were no conspicuity. It is possible that the heterogeneity and increased signal intensity of the cirrhotic liver parenchyma obscured the mild hyperintense HCC

nodules on DWI. Maybe, it also likely to be due to the limited resolution of technique for that smaller *b* values of 50 & 150/mm^2 would have provided suppression of the signal from background vessels with better contrast-to-noise ratio (CNR) and lesion conspicuity (16).

Moreover, the DWI and dynamic enhanced MR images were assessed in combination with the unenhanced T1/T2-weighted images. So the diagnostic effects of DWI and dynamic enhanced MR imaging alone could not be isolated, however, several imaging sequences in clinical practice are usually combined for diagnostic evaluation.

There are recognized limitations of our study. Firstly, we did not calculate ADC value but only evaluated the native DWI. Secondly, the 2D dynamic gradient-echo sequence might not provide greater spatial and contrast resolution compared with 3D T1-weighted sequence. Besides, there is a debate that which is better to use between breath-hold technique or a respiratory triggered version. These remain to be investigated further in future studies.

In conclusion, for focal nodular lesions in cirrhotic liver, combined diffusion-weighted imaging and conventional MR images yielded better accuracy in the detection of hepatic nodules (HDN and HCC). Diffusion-weighted MR imaging does provide added diagnostic value in the detection and characterization of HDN and HCC, and it may not be helpful for LDN and RN in cirrhotic liver.

Acknowledgements

This work was supported by the Capital Medical Development Foundation (Grant No. 2011-2015-02), the National Basic Research Program of China (973 Program) (Grant No. 2011CB707705), and the Capital Characteristic Clinical Application Research (Grant No. Z121107001012115).
Disclosure: The authors declare no conflict of interest.

References

1. Nasu K, Kuroki Y, Nawano S, et al. Hepatic metastases: diffusion-weighted sensitivity-encoding versus SPIO-enhanced MR imaging. Radiology 2006;239:122-30.
2. Taouli B, Vilgrain V, Dumont E, et al. Evaluation of liver diffusion isotropy and characterization of focal hepatic lesions with two single-shot echoplanar MR imaging sequences: prospective study in 66 patients. Radiology 2003;226:71-8.
3. Yoshikawa T, Kawamitsu H, Mitchell DG, et al. ADC measurement of abdominal organs and lesions using parallel imaging technique. AJR Am J Roentgenol 2006;187:1521-30.
4. Moteki T, Horikoshi H. Evaluation of hepatic lesions and hepatic parenchyma using diffusion-weighted echo-planar MR with three values of gradient b-factor. J Magn Reson Imaging 2006;24:637-45.
5. Taouli B, Koh DM. Diffusion-weighted MR imaging of the Liver. Radiology 2010;254:47-66.
6. Hussain SM, Terkivatan T, Zondervan PE, et al. Focal nodular hyperplasia: findings at state-of-the-art MR imaging, US, CT, and pathologic analysis. Radiographics 2004;24:3-17; discussion 18-9.
7. Mortelé KJ, Praet M, Van Vlierberghe H, et al. Focal nodular hyperplasia of the liver: detection and characterization with plain and dynamic-enhanced MRI. Abdom Imaging 2002;27:700-7.
8. Hussain HK, Syed I, Nghiem HV, et al. T2-weighted MR imaging in the assessment of cirrhotic liver. Radiology 2004;230:637-44.
9. Krinsky GA, Lee VS, Theise ND, et al. Hepatocellular carcinoma and dysplastic nodules in patients with cirrhosis: prospective diagnosis with MR imaging and explantation correlation. Radiology 2001;219:445-54.
10. Danet IM, Semelka RC, Leonardou P, et al. Spectrum of MRI appearances of untreated metastases of the liver. AJR Am J Roentgenol 2003;181:809-17.
11. Yu JS, Kim KW, Jeong MG, et al. Nontumorous hepatic arterial- portal venous shunts: MR imaging findings. Radiology 2000;217:750-6.
12. Kim JH, Kim MJ, Suh SH, et al. Characterization of focal hepatic lesions with ferumoxides-enhanced MR imaging: utility of T1-weighted spoiled gradient recalled echo images using different echo times. J Magn Reson Imaging 2002;15:573-83.
13. Parikh T, Drew SJ, Lee VS, et al. Focal liver lesion detection and characterization with diffusionweighted MR imaging: comparison with standard breath-hold T2-weighted imaging. Radiology 2008;246:812-22.
14. Vandecaveye V, De Keyzer F, Verslype C, et al. Diffusion-weighted MRI provides additional value to conventional dynamic contrast-enhanced MRI for detection of hepatocellular carcinoma. Eur Radiol 2009;19:2456-66.
15. Xu PJ, Yan FH, Wang JH, et al. Added value of breathhold diffusion-weighted MRI in detection of small hepatocellular carcinoma lesions compared with dynamic contrast-enhanced MRI alone using receiver operating characteristic curve analysis. J Magn Reson Imaging 2009;29:341-9.

16. Coenegrachts K, Delanote J, Ter Beek L, et al, Improved focal liver lesion detection: comparison of single-shot diffusion-weighted echoplanar and single-shot T2 weighted turbo spin echo techniques. Br J Radiol 2007;80:524-31.
17. Vogl TJ, Schwarz W, Blume S, et al. Preoperative evaluation of malignant liver tumors:comparison of unenhanced and SPIO (Resovist)-enhanced MR imaging with biphasic CTAP and intraoperative US. Eur Radiol 2003;13:262-72.
18. Baron RL, Peterson MS. From the RSNA refresher courses: screening the cirrhotic liver for hepatocellular carcinoma with CT and MR imaging: opportunities and pitfalls. Radiographics 2001;21:S117-32.
19. Lim JH, Cho JM, Kim EY, et al. Dysplastic nodules in liver cirrhosis: evaluation of hemodynamics with CT during arterial portography and CT hepatic arteriography. Radiology 2000;214:869-74.
20. Seki S, Sakaguchi H, Kitada T, et al. Outcomes of dysplastic nodules in human cirrhotic liver: a clinicopathological study. Clin Cancer Res 2000;6:3469-73.
21. Low RN, Gurney J. Diffusion-weighted MRI (DWI) in the oncology patient: value of breathhold DWI compared to unenhanced and gadolinium-enhanced MRI. J Magn Reson Imaging 2007;25:848-58.
22. Kiryu S, Watanabe M, Kabasawa H, et al. Evaluation of super paramagnetic iron oxide-enhanced diffusion-weighted PROPELLER T2-fast spin echo magnetic resonance imaging: Preliminary experience. J Comput Assist Tomogr 2006;30:197-200.
23. Koh DM, Brown G, Riddell AM, et al. Detection of colorectal hepatic metastases using MnDPDP MR imaging and diffusion-weighted imaging (DWI) alone and in combination. Eur Radiol 2008;18:903-10.
24. Lee MH, Kim SH, Park MJ, et al. Gadoxetic acid-enhanced hepatobiliary phase MRI and high b-value diffusion-weighted imaging to distinguish well-differentiated hepatocellular carcinomas from benign nodules in patients with chronic liver disease. AJR 2011;197:W868-75.
25. Le Moigne F, Durieux M, Bancel B, et al. Impact of diffusion-weighted MR imaging on the characterization of small hepatocellular carcinoma in the cirrhotic liver. Magn Reson Imaging 2012;30:656-65.
26. Park MJ, Kim YK, Lee MH, et al. Validation of diagnostic criteria using gadoxetic acid-enhanced and diffusion-weighted MR imaging for small hepatocellular carcinoma (≤2.0 cm) in patients with hepatitis-induced liver cirrhosis. Acta Radiol 2013;54:127-36.
27. Sandrasegaran K, Tahir B, Patel Al, et al. The usefulness of diffusion-weighted imaging in the characterization of liver lesions in patients with cirrhosis. Clin Radiol 2013;68:708-15.

Cite this article as: Chen ML, Zhang XY, Qi LP, Shi QL, Chen B, Sun YS. Diffusion-weighted images (DWI) without ADC values in assessment of small focal nodules in cirrhotic liver. Chin J Cancer Res 2014;26(1):38-47. doi: 10.3978/j.issn.1000-9604.2014.01.07

